Microstructural and interface properties of aluminium alloy coatings on alumina applied by friction surfacing

H.B. Atil[a,b,c,*], M. Leonhardt[b], R.J. Grant[c], S.M. Barrans[a]

[a]*Huddersfield University, Dept. Computing and Engineering, United Kingdom*
[b]*Kempten University of Applied Sciences, Dept. Mechanical Engineering, Germany*
[c]*Western Norway University of Applied Sciences (HVL), Dept. Mechanical and Marine Engineering, Norway*

Abstract

Two large groups of materials, namely metals and ceramics, are used in mass quantities in today's industry because of their outstanding properties. To achieve higher product performance dissimilar materials need to be combined in assemblies, but their joining is challenging. Using friction surfacing technology Al_2O_3 ceramic substrates were coated with an aluminium alloy (AlMg4.5Mn0.7). Earlier research by the authors suggested that two major bonding mechanisms, namely mechanical interlocking and van der Waals forces, are responsible for the bonding strengths achieved between the coating and the substrate. Further SEM, STEM, HRTEM and EDX analyses at a sub nanometer resolution were conducted and are presented in this paper. These analytical methods revealed that the aluminium coating and the Al_2O_3 grains form a sharp boundary without evidence of either a chemical reaction or diffusion at the interface and suggest that the main bonding mechanisms for the Al/Al_2O_3 system are van der Waals forces. In addition, mechanical interlocking may serve to hold in position the interface surfaces, to preserve their close proximity, allowing the van der Waals forces to persist.

Keywords: friction surfacing, friction coating, aluminium alloy, alumina, ceramics, van der Waals, mechanical interlocking

*Corresponding author. Tel.: +49 (831) 2523233
Email address: hasan.atil@hs-kempten.de & hasan.atil@hud.ac.uk & hbah@hvl.no (H.B. Atil)

1. Introduction

Increasing demands for high performance materials leads to a sustained pressure for the development of new materials, pushing physical and mechanical limitations to new levels. Parts with locally differentiated material properties allow a tailored adaptation to the desired application profiles. Designs may require components to be fixed in specific locations or combined with other parts. According to Martinsen et al. [1] dissimilar materials with different properties are jointly used to achieve higher product performance in several industries already (e.g. automotive, aeronautics, marine applications). But joining these dissimilar materials, for instance ceramics with metals, for further use in assemblies is challenging [2]. Metallized ceramics find their largest field of application in electrical engineering, e.g. as insulators, diffusion pumps, thyristor and diode housings. Joining these dissimilar materials is difficult and technologies currently used are complex and relatively costly. According to Asthana and Sobczak [3] coating-substrate adhesion is promoted by wettability and develops physical, chemical and mechanical interactions. Chemical reactions at the surface are especially difficult to achieve for ceramic materials, due to their strong ionic-covalent bonding types (e.g. Al_2O_3 mostly ionic, Si_3N_4 mostly covalent) which hold the atoms together [4]. Whereas ceramic coatings applied on metal substrates serve the purpose of modifying the surface structure for increased wear resistance and hardness [5], metal coatings applied to ceramic substrates provide an intermediate adhesion layer affording a means to bond with new layers or other parts.

In this research work a new low-cost, reliable and robust coating technique for ceramics based on friction surfacing (FS) was developed. Friction surfacing is a coating method in which, predominantly, metal substrates are coated with metals [14]. In earlier work by the authors [6] ceramic substrates (Al_2O_3) were coated with an aluminium alloy (AlMg4.5Mn0.7) generating coating thicknesses of 200μm and bonding strengths of 47MPa. Initial tests revealed that the interface temperature can reach up to approximately 580°C. At this temperature the coating material, which was in a viscoplastic state, flowed into the pores forming mechanical bonds by interlocking. This was calculated to account for 16% of the bonding strength [6]. One may come to the assumption that by the viscoplastic flow of the aluminium coating moving into the pores of the substrate air could be pressed out of the cavities and create a pressure difference to the surrounding atmosphere causing adhesion through suction. Experiments conducted by Budgett [7], bringing two metal surfaces in close contact in vacuum, refute this theory concluding that molecular attraction is the main driving

force for adhesion. This is also confirmed for ceramic-metal interfaces in a recent publication by Miyoshi and Abel [8] stating that when a clean metal is brought into contact with a clean ceramic surface in ultrahigh vacuum, strong bonds between the two materials form. Popov [9], Lipkin et al. [10] and Deng et al. [11] try to quantify the bonding mechanisms in metal-ceramic systems and come to the conclusion that: as the interface surfaces may be in very close proximity van der Waals forces could come into play, so contributing to metal-ceramic adhesion. To date, friction surfacing of ceramics has seen little research attention, except for one article in a trade magazine of The Welding Institute (TWI) in Abington, Cambridge UK [12] and a recently published article in the peer-reviewed journal Coatings [13]. TWI [12] describes the successful deposition of aluminium onto an alumina substrate on their webpage. These tracks of aluminium are only a few millimetres wide and less than 50µm thick. A similar approach was used by Chmielewski et al. [13], investigating the properties of titanium (Ti) coatings on an aluminium nitride (AlN) substrate deposited by friction surfacing. Coating thicknesses up to 7 μm were reported as having been achieved. Friction surfacing of large surface areas or reports of achieving a coating thickness in the millimetre range, so producing material composites, is not as yet possible. There are no known publications in this area other than what is listed here.

In the friction surfacing process, a rotating disc or rod of coating material is pressed against a substrate surface. The heat generated by friction weakens the bonds between the atoms and decreases the yield strength [15]. This leads to a change in the flow properties of the coating material (i.e. plasticisation). The introduction of relative transverse motion along the substrate surface results in material being deposited [16]. The generated heat and applied pressure leads to the formation of new bonds between the two materials. Figure 1 shows a coated Al_2O_3 specimen with the matching rod.

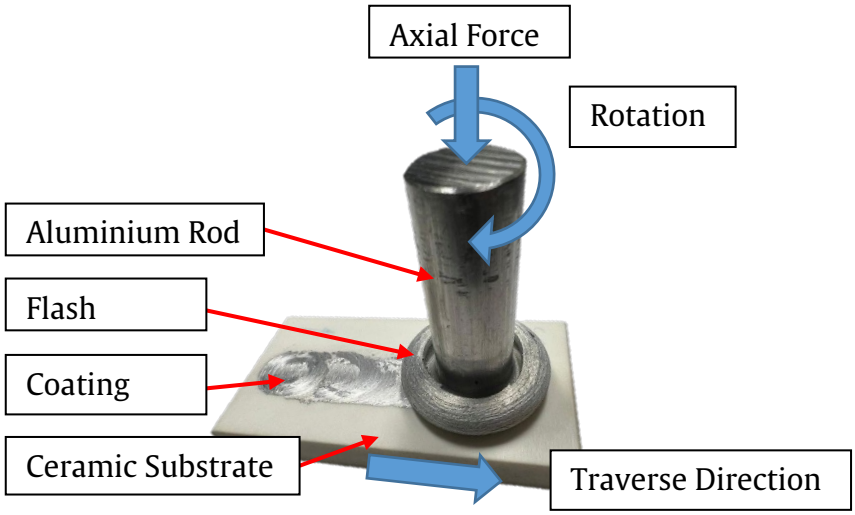

Fig. 1. Friction surfaced Al_2O_3 specimen.

Friction surfacing of ceramics is a simple and fast coating process. Short coating times enable the process to be integrated within automated production lines. Thick layers can be produced in seconds and realise bonding strengths similar to current metallizing methods such as magnetron sputtering (i.e. physical vapour deposition) [23] and thermally sprayed coatings [24].

A review publication by Gandra et al. [14] gives a broad insight into the topic of friction surfacing and acting mechanisms. Achieved bonding types differ significantly, depending on the process parameters and material combination used. According to Bedford et al. [17] the bond between high speed steel coatings and carbon steel substrates applied by friction surfacing is formed by diffusion. This is a result of the force applied and the temperature reached at the interface. Looking at combinations of dissimilar materials with different strengths, mechanical interlocking can occur. The applied force and temperature can deform the substrate in such a way that the coating rod forms dovetail shaped indentations on the surface and creates a bond by interlocking structures [18]. Interlocking can also occur when the coating material, in its visco-plastic state, flows into the pores of the substrate forming anchor-points. In the work of Chandrasekaran et al. [19] who studied the interface of mild steel substrates coated with Inconel alloys, evidence of reaction products forming at the interface can clearly be seen in microscope images. It is stated that these chemical bonds increase the bonding strength significantly. As described by Butt et al. [20] this is the most effective bonding mechanism, with bonding strengths that are usually excellent; this can also be desirable for

friction surfaced coatings. Despite the fact that van der Waals forces are not mentioned in friction surfacing publications it plays a major role in ceramic-metal interfaces [11, 21]. These forces arise whenever two materials come in close contact with each other and result from dipole interactions. It is important to know that they also act between different materials and depend only on the contact distance, making them universal in interaction [22].

The research described in this paper aimed to determine the prevailing bonding mechanism for when alumina is friction surfaced with an aluminium alloy.

2. Experimental setup and method

The experimental setup is shown in Figure 2. A standard milling machine (DMG Mori Co., Germany, Model: Maho MH700) was adapted to apply metal coatings onto ceramic substrates.

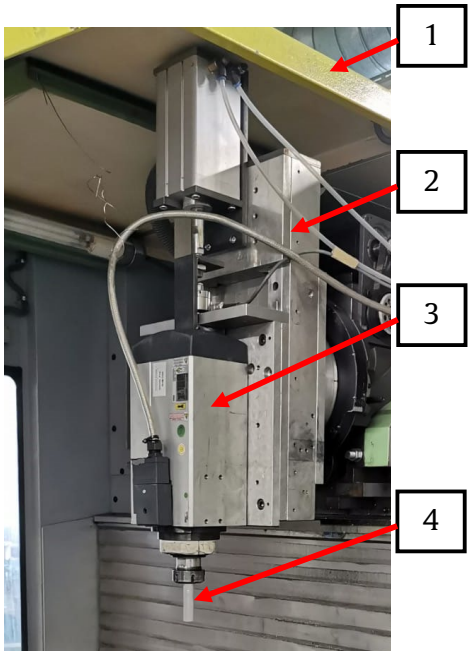

Pos.	Description
1	Converted machine
2	Slide
3	Spindle
4	Coating rod

Fig. 2. Experimental setup.

To clamp the ceramic substrates a special clamping device was designed and manufactured (see Figure 3) [25].

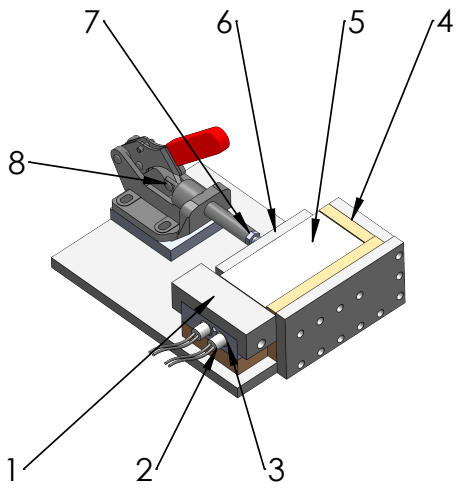

Pos.	Description
1	Starting plate
2	Heating cartridge
3	Heating plate
4	Insulation
5	Ceramic substrate
6	Clamping jaw
7	Head screw
8	Pull-down clamp

Fig. 3. Clamping device design.

Jahanmir [26] gives an overview of ways and means of machining and clamping ceramic materials. He states that when clamping ceramics the specific characteristics of the material have to be taken into account as local load peaks could induce cracking. Thus, for better force distribution the ceramic substrate was clamped on the long side using a pull-down clamp locked into a clamping jaw.

In previous work by the authors micro-cracking in the substrate caused by thermal shock was observed [6]. It was noted that an abrupt increase in temperature can lead to a higher thermal stress causing substrate failure. To reduce the thermal shock on the ceramic substrate the process of pressing the rotating coating rod was initiated directly on the substrate; which was in contrast to previous work, where a *starting plate* was employed.

Figure 4a and Figure 4b shows two thermal profiles with and without the use of a starting plate.

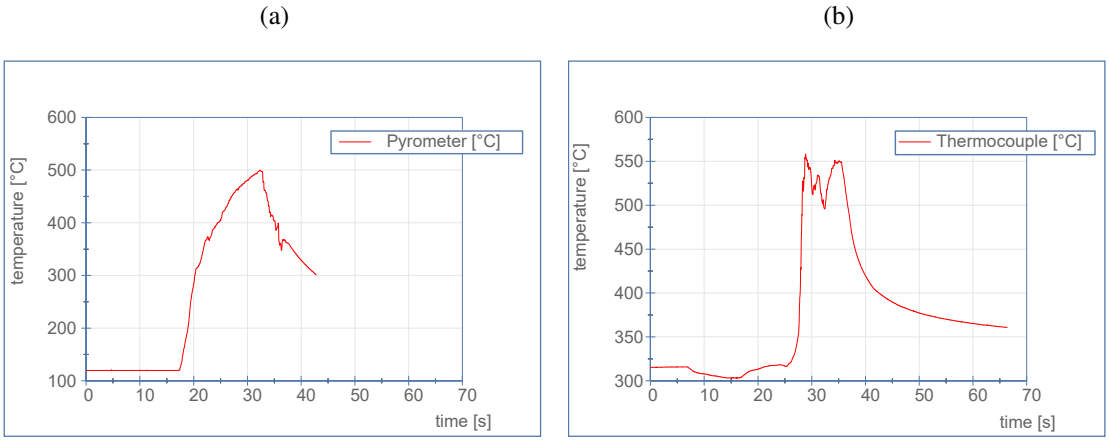

Fig. 4. Thermal profiles of specimens coated (a) without the use of a starting plate and (b) with the use of a starting plate.

For the first test (see Figure 4a) the temperature was recorded with the use of a pyrometer aimed at the interface between the coating rod and the substrate. For the second test shown in Figure 4b a thermocouple was embedded at the surface of the substrate. It can be seen that the increase in temperature for the specimen without the use of a starting plate (Figure 4a) is slower over time leading to an additional heating of the substrate. Whereas the temperature rise for the specimen with the use of a starting plate (Figure 4b) is sharp and abrupt. Thus, the use of a starting plate was omitted for this parametric study.

Also, preliminary tests revealed that preheating the specimens to a temperature of 150°C reduced the probability of fracture. Thus, two high performance heating cartridges (Tuerk & Hillinger GbmH, Germany, Model: HLP 125099) were used to preheat the specimens.

2.1. Material selection and preparation

It is desirable that the coating material should be a weldable alloy which would allow for joining assemblies in subsequent processes. According to Ostermann [27] the weldability, corrosion resistance and ductility of the EN AW-5xxx group of alloys is excellent. In addition, the chosen alloy, EN AW-5083 (AlMg4.5Mn0.7) has a high strength with the manganese and magnesium content supporting chemical bonding by forming $MnAl_2O_4$ and $MgAl_2O_4$ spinel at the interface.

For the substrate material Al_2O_3 was chosen. Aluminium oxide is one of the most widely used technical ceramics [28]. Due to its high corrosion resistance it is used in the chemical industry for

corrosion protection and furnace lining [29]. It is well known for its good mechanical properties and thermal stability. It shows temperature resistance up to 1850°C and at the same time exhibits excellent fracture and wear resistance with high stiffness [30]. Larger quantities are readily available and inexpensive to obtain.

For the experiments aluminium alloy rods with dimensions of ∅ 20 x 80 mm as a coating material, and 92% alumina plates (i.e. 92% pure Al_2O_3 and 8% additives) as a substrate material with dimensions of 150 x 50 x 13 mm were used. The ceramic substrate surfaces were ground and chamfered. Before starting the coating process all material surfaces were degreased.

3. Results and Discussion

Results on achieved coating thicknesses and bonding strengths were published in earlier work by the current authors [6]. This section will give an insight into the acting bonding mechanisms.

It was reported that temperatures can reach up to approximately 580°C during the coating process. Analysis of the interface showed no clear evidence for intermetallic compounds with investigations turning towards van der Waals forces as the main source for the achieved bonding strength. These forces can be calculated by determining the distance between the two close-contact bodies [31] and for two flat surfaces the following equation can be used [32, 33]:

$$P(D) = \frac{H}{6 \cdot \pi \cdot D^3} \tag{1}$$

where $P(D)$ is the bonding strength, H is the Hamaker constant and D the distance between the two surfaces.

The Hamaker constant is a coefficient relating to the force between particles interacting through van der Waals forces [34], it is dependent on the materials in contact and the separation medium. It assesses the magnitude of the van der Waals interactions whereby the van der Waals forces are directly proportional to the Hamaker constant (see equation 1). According to Bergström [35] the Hamaker constant can be estimated by the dielectric properties of the interacting materials and the separation medium. Unknown Hamaker constants can be approximated by combining known ones by employing equation [32]:

$$H_{132} = (\sqrt{H_{11}} - \sqrt{H_{33}})(\sqrt{H_{22}} - \sqrt{H_{33}}) \tag{2}$$

$$H_{132} = \sqrt{H_{11} \cdot H_{22}} \tag{3}$$

where H_{11} is the Hamaker constant of material one, H_{22} of material two, H_{33} of the medium separating the two materials and H_{132} is the combined constant. Note that the Hamaker constant for a vacuum and air is zero, and thus the Hamaker constant for the separation medium H_{33} may be dropped from the equation.

The Hamaker constants for Al_2O_3 and molten aluminium can be taken from literature (i.e. $H_{Al_2O_3} = 140 \cdot 10^{-21} J$[36], $H_{Al} = 266 \cdot 10^{-21} J$[37]); with H_{Al/Al_2O_3} calculated from equation 3 as $254 \cdot 10^{-21} J$.

Using equation 1 and the combined Hamaker constant, the adhesion tension can be determined as a function of the separation distance: this was computed and plotted in Figure 5. First estimates of the van der Waals forces suggest that these interactions will manifest themselves at a nano-meter scale.

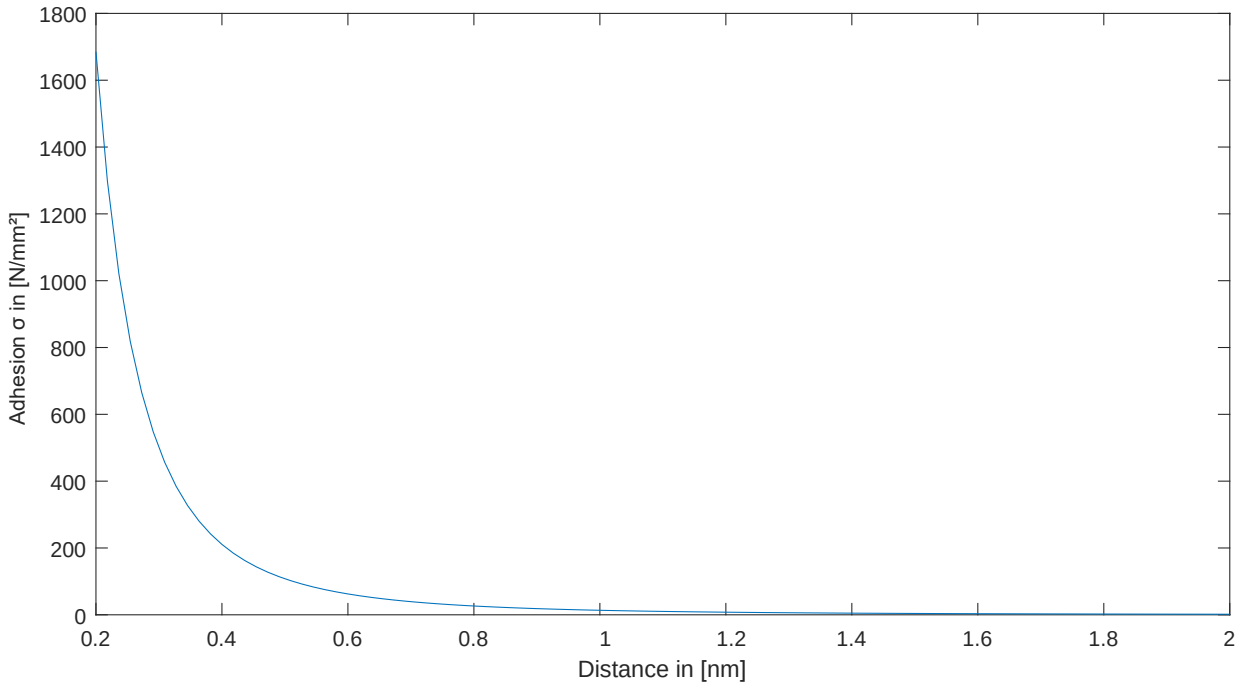

Fig. 5. Van der Waals forces.

Due to the combination of a hard and brittle material (Al_2O_3) and a ductile material (Al-alloy),

preparation of specimens to allow inspection of the interface was found to be challenging. When polishing, smearing of the aluminium onto the alumina substrate was an issue making it difficult to analyse the interface properly. Therefore, specimens were prepared by using a combination of a focused ion beam milling instrument with a scanning electron microscope (FIB-SEM), and analysed for occurring elements by Energy-dispersive X-ray spectroscopy (EDX). Specimens of different density and ductility were prepared without smearing, and surfaces were polished by milling at a nanometre scale.

For SEM imaging and EDX analysis a Zeiss Auriga 60 with an Ametek EDAX Octane Elect+ Detector was used, whilst for FIB-SEM preparation and analysis a Zeiss NVision 40 was employed.

3.1. Microscopic and EDX analysis

Coated specimens have been cut, embedded in epoxy and ion milled for high-resolution imaging which would not be possible by polishing the specimens using traditional methods alone. Figure 6a-6d shows the coated specimen after initial slicing for better handling and the cut-off part for analysis. Figures 6e and 6f show the specimen before and after ion milling (IM), respectively. As can be seen the surface structure of the specimen is much smoother after ion milling and shows a more polished appearance. This is much more apparent at a microscopic level and was done to help identify bonding mechanisms in greater detail.

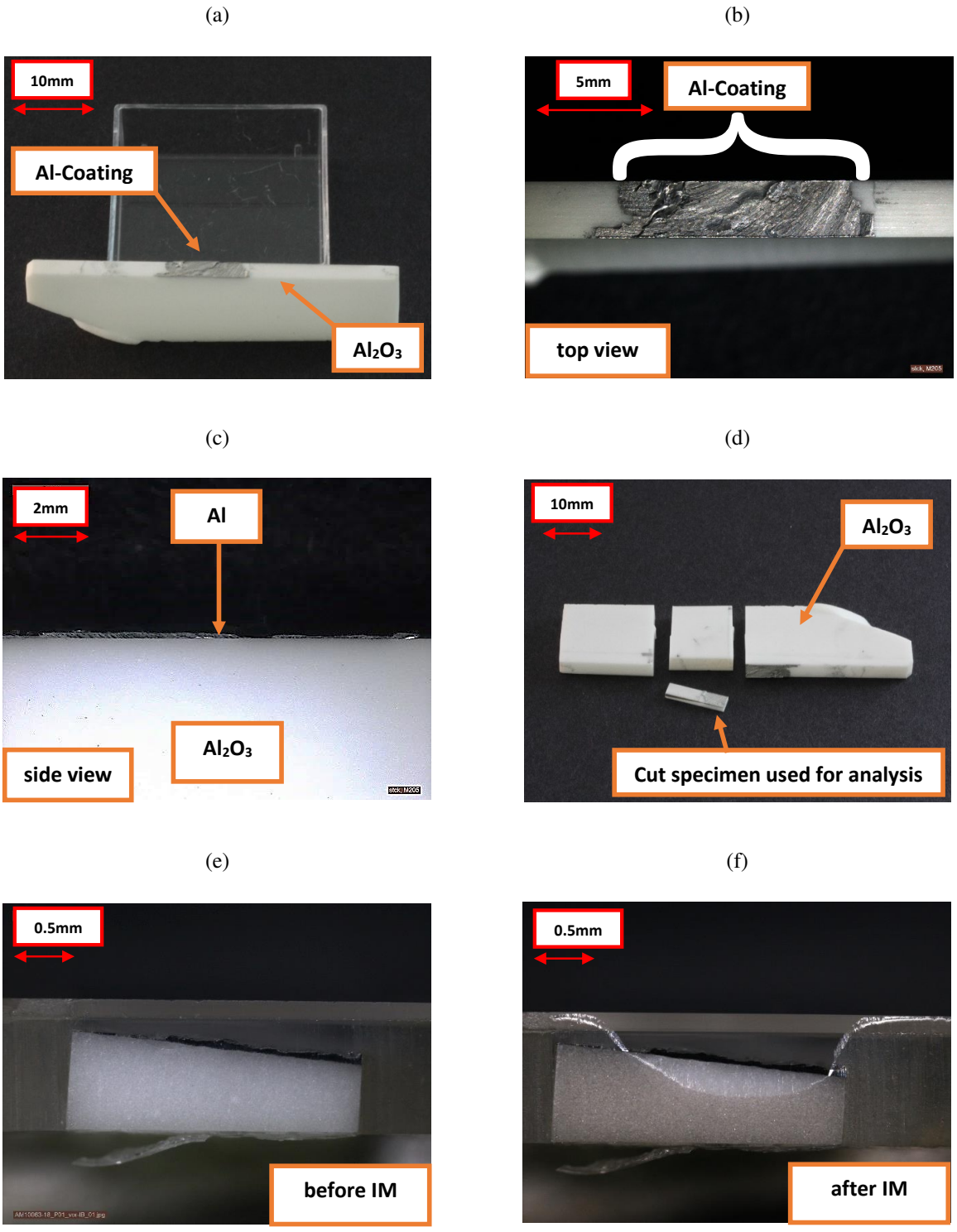

Fig. 6. Al_2O_3 specimen (a) after initial slicing, (b) top view before cutting, (c) side view before cutting, (d) cut specimen for analysis, (e) before and (f) after ion milling.

190 Looking at Figure 7 the undesired crack formation reported in [6] can be seen spanning from

the LHS to the RHS of the image. Shifting the focus to the substrate, not only can individual alumina grains be identified; but also the size and grain structure of the coating material is exposed. Examining the coated layer it is apparent that the grain size near the surface of the coating is much smaller than at the metal-ceramic interface. According to Bararpour et al. [38], and by way of comparison - who studied thermal and mechanical reactions during friction surfacing of aluminium alloy substrates using aluminium alloy rods for the coating, the prevailing high temperatures and pressure leads to dynamic recrystallisation of the coating material. In this case, due to the high cooling rates at the interface, a finer grain size can be observed at the interface than near the surface at the top of the coating. This is in contrast with what was observed in *this* study. Because of the low thermal conductivity of the Al_2O_3 substrate and the insulation surrounding the substrate in the clamping device (see Figure 3), heat transfer is restricted beneath the ceramic substrate. The surface of the coating, on the other hand, is in contact with the ambient air and can therefore radiate heat leading to an abrupt temperature drop. As mentioned by Humphreys et al. [39] one major factor affecting grain growth during dynamic recrystallisation is temperature and that ”significant grain growth is often found only at very high temperatures”. Transferring this knowledge to the conducted experiments it becomes evident that the temperature at the interface does not change as abruptly as on the coating surface; giving more time for grain growth. A smaller grain size may lead to an increase in tensile strength [40] of the coating material and will be part of future investigations.

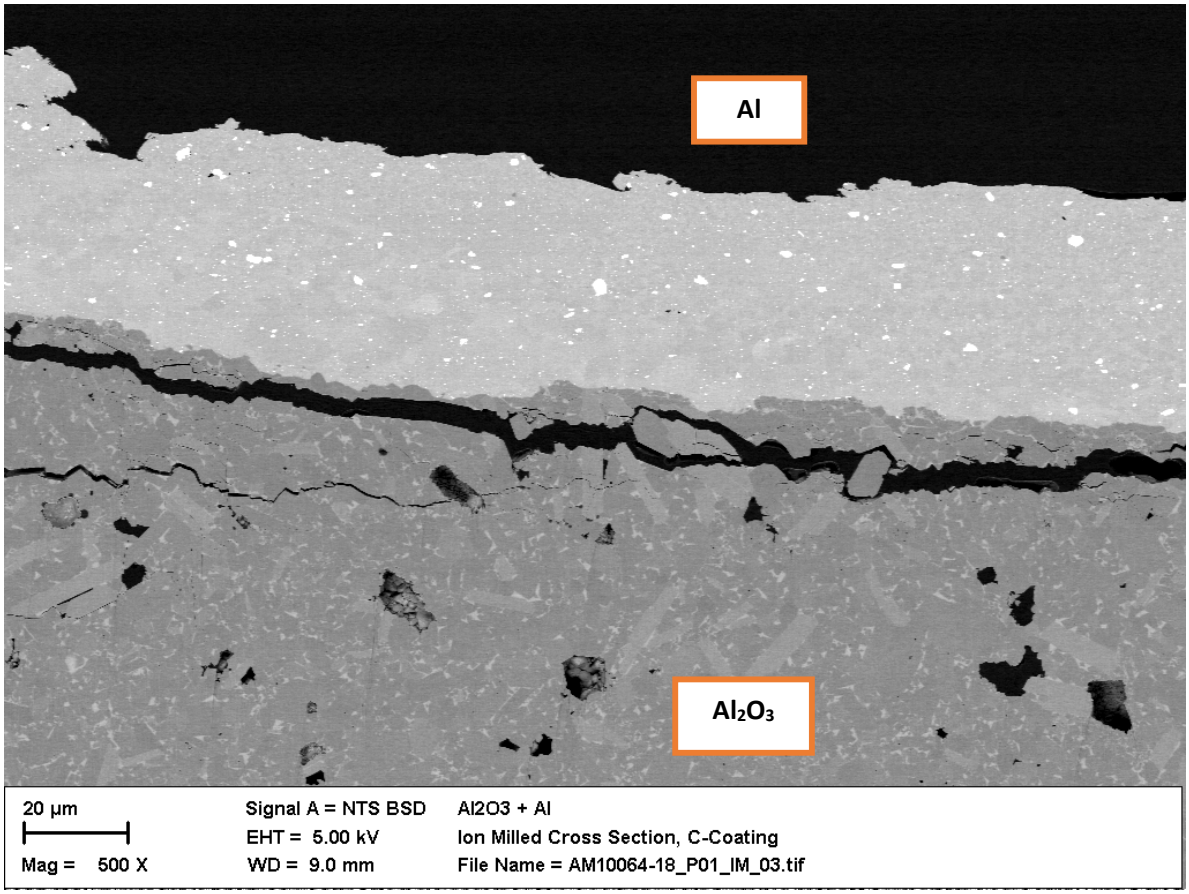

Fig. 7. Ion-milled cross section of Al_2O_3 + Al coating.

Examining the aluminium coating and ceramic substrate at different spots by EDX analysis (Figure 8) reveals intermetallic compounds (i.e. $Al_6(Fe,Mn)$) as blocky particles present in the aluminium alloy, an example of which can be identified at spot 2. These form due to the high Mn content in the alloy and increase the strength of the material [41]. Also, magnesium oxide, silicon oxide and calcium oxide (i.e. spot 5) accumulate at the grain boundaries of the ceramic substrate (i.e. spot 3 shows a region of the substrate). These additives lower the sintering temperature and are used during production [42].

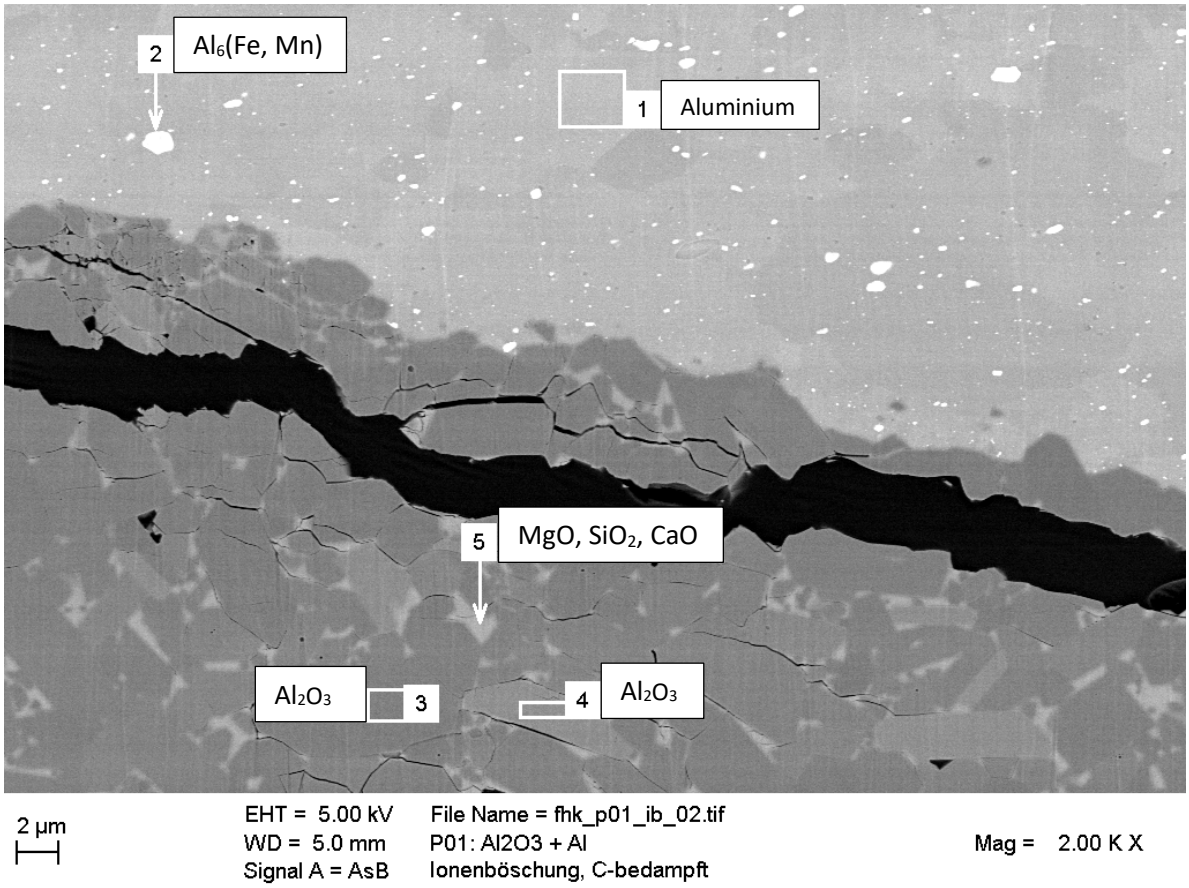

Fig. 8. Cross section of Al_2O_3 + Al coating with marked EDX analysis spots.

According to Imanaka [43] these glassy-phases are used for metallizing Al_2O_3 with nickel by chemical reaction of the glassy-phases with the applied Mo-Mn-paste forming anchor points. Looking again at Figure 8 some grain boundaries are exposed to the aluminium coating and could react in the same fashion to form a solid bond between the glassy-phase and the metal. According to Berek et al. [44] who studied interfacial reactions of Al_2O_3 particle reinforced 6061 aluminium alloys, in their work no reaction products were found at the particle/matrix interfaces in the as-cast state. Consistent with these findings Zhou et al. [45], who studied interfacial reactions of metal-matrix composites consisting of alumina preforms infiltrated with aluminium-manganese-alloys, reaction products at the interface were found to be rare and that structureless interfaces between alumina and aluminium were a more typical occurrence. Similar studies by Yu et al. [46] confirm

these results. Using higher magnifications (Figure 9) no interfacial reactions are evident. The sharp boundaries of the aluminium oxide grains are completely enclosed by aluminium showing no evidence of a gap or reaction zone.

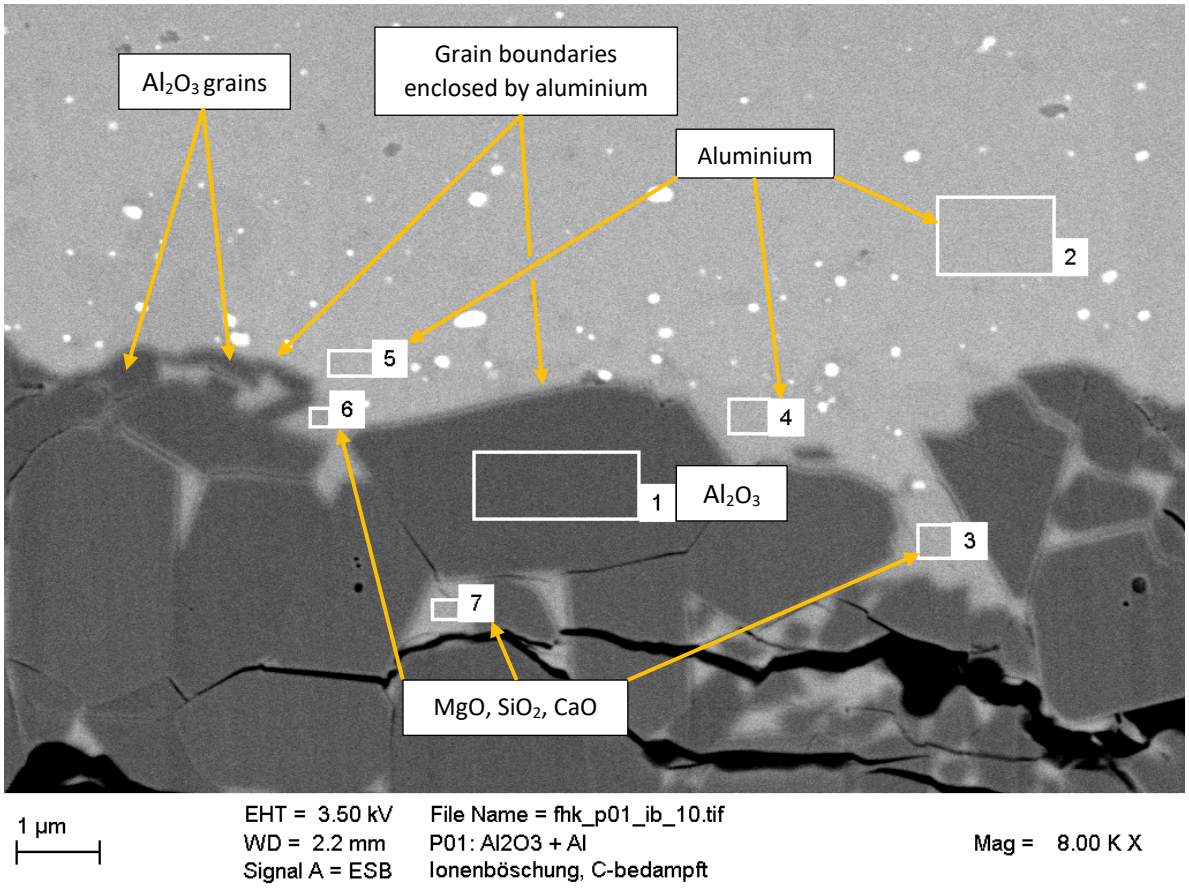

Fig. 9. Higher magnification image of aluminium oxide grains and boundaries.

Changing the contrast of the image serves to emphasise this point (Figure 10).

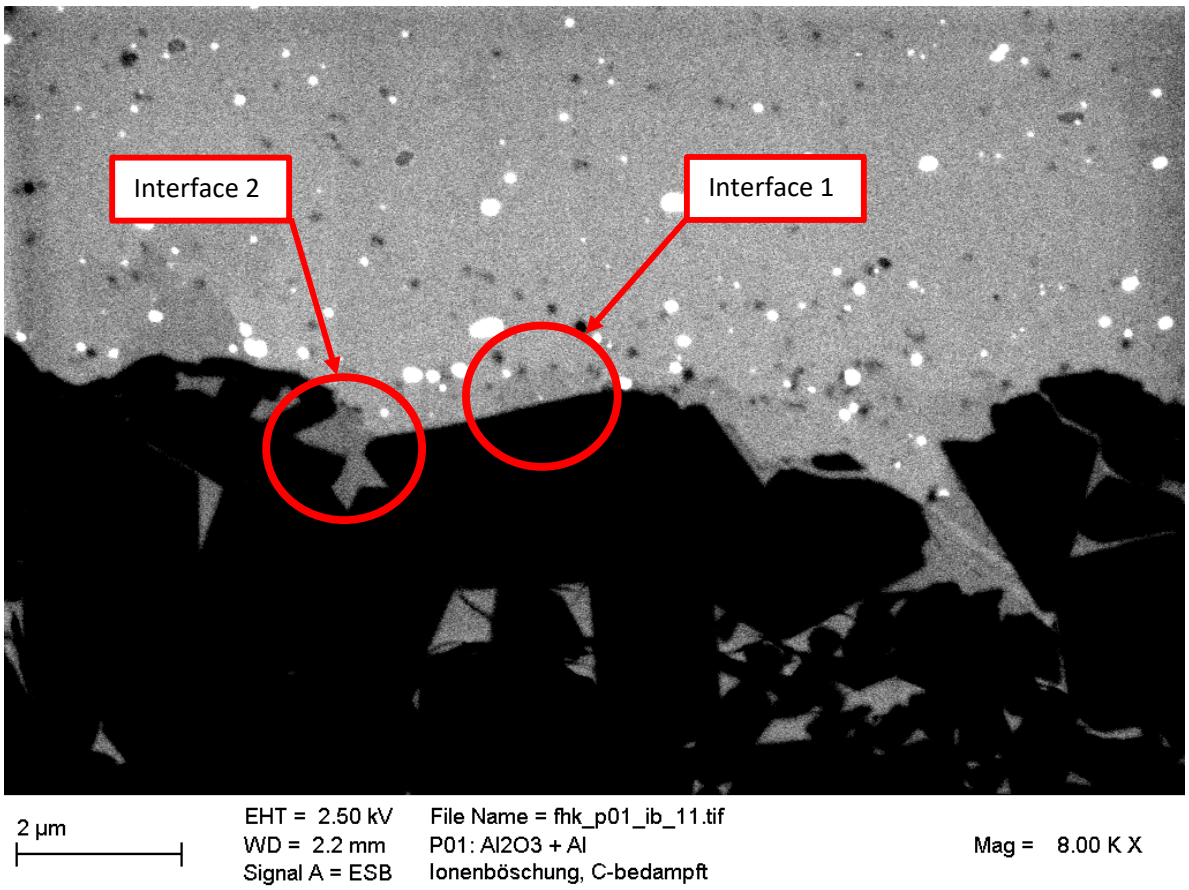

Fig. 10. High contrast image of aluminium oxide grains and boundaries.

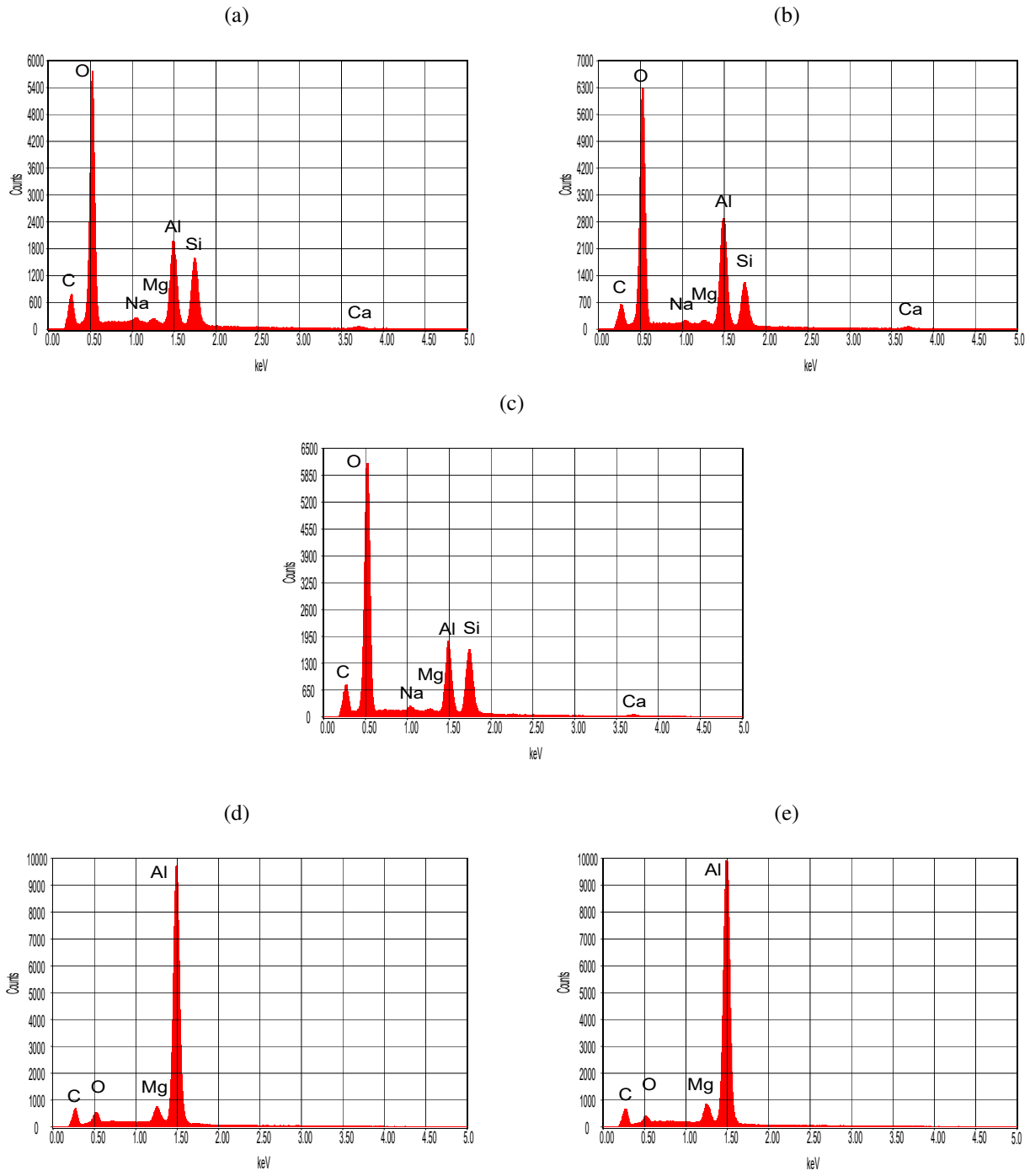

Fig. 11. EDX analysis of spots (a) 3, (b) 6, (c) 7, (d) 4 and (e) 5 shown in Figure 9.

EDX analysis at different locations was conducted (see Figure 9 for spot positions). Comparing spots 3, 6 and 7 (EDX profile in Figure 11a, 11b and 11c respectively) reveals that these areas are accumulations of sintering additives which form the glassy-phase; cross-checked at spots 4 and 5

(Figure 11d, 11e). Interestingly spot 3 and 6 have been exposed to the aluminium coating forming a new interface. Shifting focus back to the higher contrast image (Figure 10) it can be seen that at these spots the glassy-phase and the aluminium coating form a sharp edge distinguishable by the darker and lighter grayscale, but show no reaction zone in between. This analysis of the interface is in line with literature where no reaction zone between Al_2O_3 grains and aluminium could be identified [45, 46].

Further transmission electron microscopy (TEM) analysis has been conducted to identify active binding mechanisms. For this purpose a TEM (Carl Zeiss Libra 200 Cs, with an acceleration voltage of 200 kV) was used. The integrated scanning transmission electron microscope (STEM) and high resolution TEM (HRTEM) mode was used for imaging at higher magnifications. EDX was performed on the sample using a detector from Oxford Instruments attached to the TEM.

To accommodate for the induced stress on the material during TEM preparation a specimen with a high bonding strength was selected. Figure 12a shows a coated specimen, already cut to a smaller size, with a bonding strength of 44.27 MPa. For TEM analysis samples must be prepared to be as thin as possible (i.e. lamella), so that the electrons can pass through the sample for imaging. This was done by using a FIB-SEM for cutting out the sample and polishing the specimen by ion milling. The area marked in red (Figure 12b) was used to prepare the lamella.

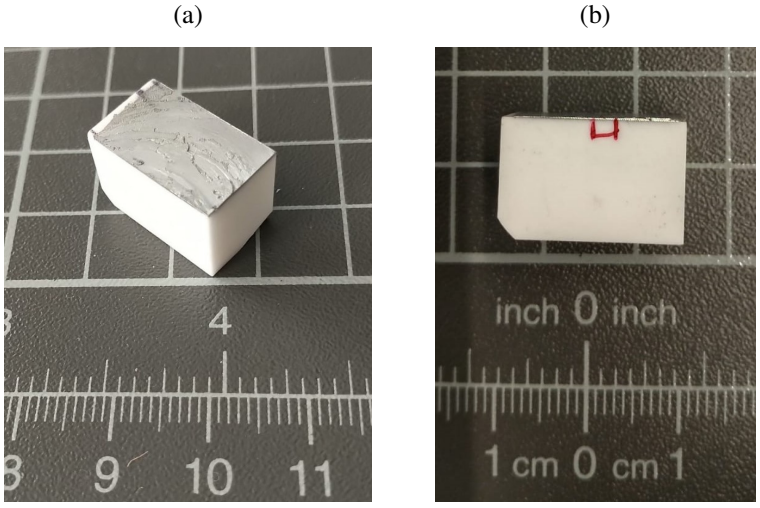

Fig. 12. (a) Image of coated specimen, and (b) marked area for lamella.

During the thinning process pores and cracks within the Al_2O_3 substrate and the aluminium part were observed (see Figure 13a). Due to the internal stress and brittle nature of the specimen the

central region was reinforced by depositing platinum onto the frail surface. Further thinning down of the specimen was carried out on the left and right side of the part.

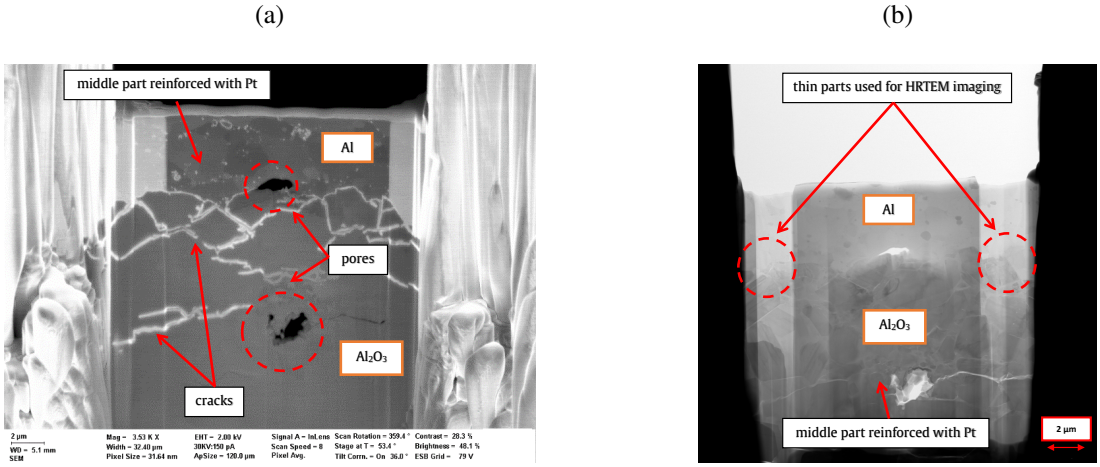

Fig. 13. (a) SEM image showing pores and cracks, and (b) STEM image showing thinned parts and region for HRTEM study.

Figure 13b shows a STEM image of the finished lamella with the marked area for the HRTEM study. The left and right side of the specimen was thinned down to 50nm whereas the middle part was used as reinforcement with a thickness of 100nm. By using HRTEM imaging the atomic structure at the interface was examined in detail. Figures 14a and 14b show images of the Al_2O_3 grain boundary and aluminium interface. At a scale of 5nm no reaction zone is visible. The lattice structure of the Al_2O_3 grains can be seen to change abruptly into the lattice structure of the aluminium. Magnifying the interface to a 1nm scale (Figure 14c) the distance between the Al_2O_3 grain and the aluminium coating could not be identified, concluding that the separation distance is lower than the scale factor.

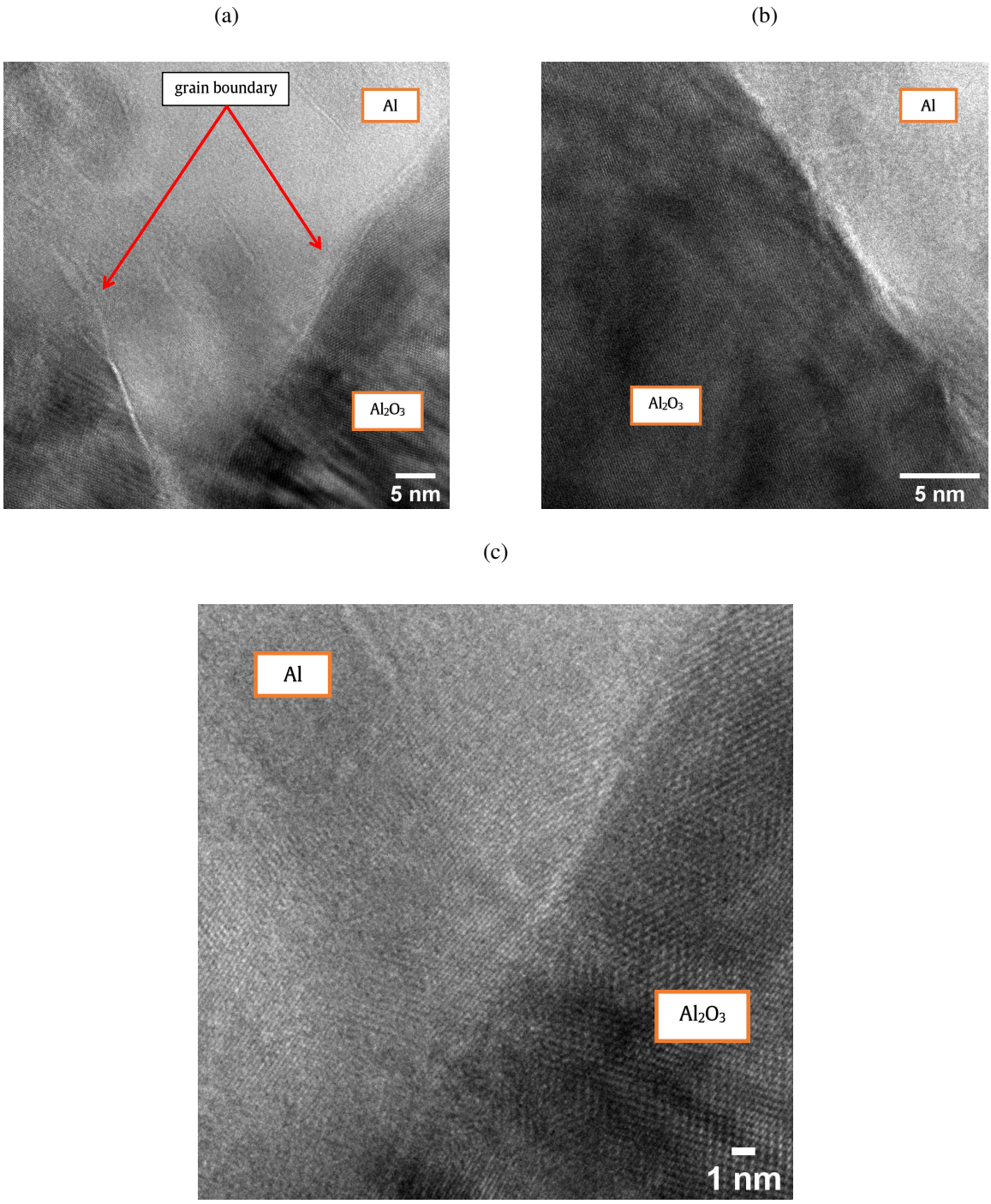

Fig. 14. HRTEM image of (a) aluminium between two Al_2O_3 grains, (b) different spot of aluminium and Al_2O_3 grain, and (c) magnification of interface.

One thing that stands out on closer inspection of the lattice structure is the partially amorphous state of the aluminium coating. According to Ojovan and Lee [47] liquid-glass transition

is observed in various types of liquids including metals. If the cooling rate is high enough crystallisation can be avoided and the metal exhibits a disordered atomic structure. These amorphous metals show higher strength and ductility than their lattice structured counterparts, but are difficult to manufacture [48]. As reported by Suryanarayana [49] amorphous alloys can be produced by mechanical alloying which is a processing technique involving repeated cold welding, fracturing and rewelding of powder particles. Transferring this procedure to friction surfacing, a similar phenomenon can be observed. The coating material is rubbed against the substrate surface where the microscopic peaks and valleys make contact and form micro-bonds. Fracture of these micro-bonds leads to heat generation and local melting of the material due to thermal spikes. Because of the applied axial force, grains are crushed into finer grains and the partial melting of the material leads to the dissolving of grain boundaries: dynamic recrystallization occurs. During deposition rapid cooling of the quasi liquid layer takes place producing fine grains in the coating. The combination of repeated crushing and recrystallizing of the grains, then rapid cooling at the interface, could lead to forming of partially amorphous aluminium as show in Figure 15.

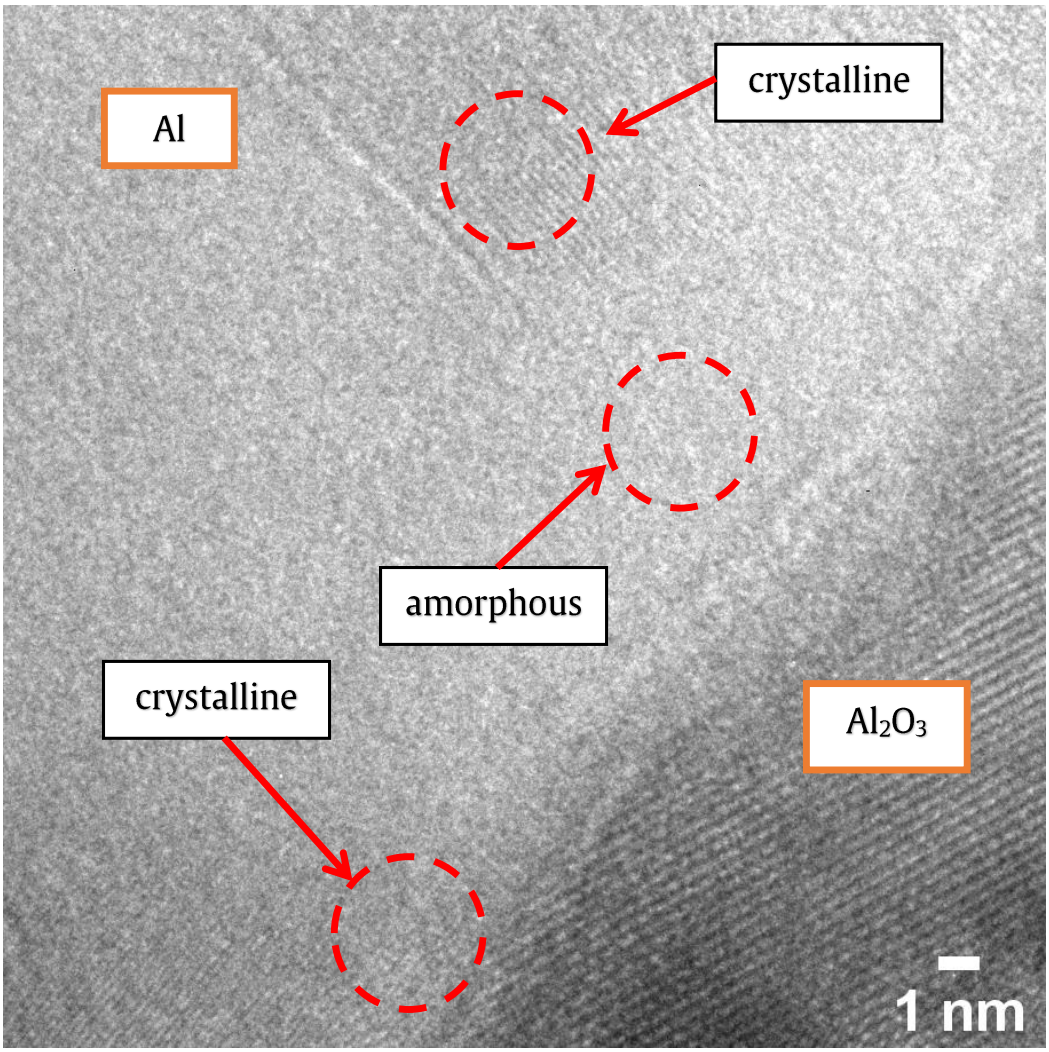

Fig. 15. Atomic structure of Al coating.

Reflecting on the findings above it can be said that van der Waals forces are the main binding mechanisms for the Al/Al_2O_3 system. Taking into account the mechanical interlocking portion of 16% [6] and using equation 1 the distance D for a given bonding strength (e.g. 44.27 MPa) can be calculated as follows:

$$D = \sqrt[3]{\frac{H}{6 \cdot \pi \cdot P}} = \sqrt[3]{\frac{254 \cdot 10^{-21}[Nm]}{6 \cdot \pi \cdot [44.27 \cdot 10^{6}[N/m^2]) \cdot (1 - 0.16)]}} = 0.713nm \tag{4}$$

Because of the reciprocal exponential relationship of the distance D to the bonding strength

285 $P(D)$ an increase in the separation distance will have an exponentially negative effect on the bonding
286 strength. It can be conjectured that the mechanical interlocking may serve to hold in position the
287 interface surfaces, to preserve their close proximity, allowing van der Waals force to persist. Also
288 interlocking may prevent transverse relative displacement between the two surfaces which would
289 prevent roughness in the contacting surfaces from increasing the separation distances. Even though
290 the pores only account for 16% of the bonding strength, their influence on the van der Waals forces
291 and their persistence should not be underestimated.

4. Conclusion

In earlier experiments alumina specimens were coated with aluminium showing encouraging results for the achieved bonding strengths and coating thicknesses [6]. The binding mechanisms discovered could not fully explain the high adhesion forces obtained. By using additional microscopic analysis methods the remaining bonding mechanisms have been identified.

- Analysis of the joint zone shows no evidence of chemical reactions (inter-metallic compounds) or diffusion.
- STEM and HRTEM analysis shows that the aluminium and the Al_2O_3 grains form a sharp boundary without evidence of a reaction zone.
- Despite the use of high resolution TEM imaging at a sub nano-meter scale the separation distance between the Al_2O_3 grains and the aluminium coating could not be identified, concluding that the distance is lower than the scale factor of 1 nm.

It can be said that van der Waals forces are the main binding mechanisms for the Al/Al_2O_3 system, however the influence of mechanical interlocking on the van der Waals forces and its persistence should not be trivialised.

5. Acknowledgement

This research work was funded by the Dobeneck-Technologie-Stiftung, Germany. The authors gratefully acknowledge the financial support received.

6. Declaration of Conflicting Interests

Mr. Atil reports grants from Dobeneck-Technologie-Stiftung during the conduct of the study. The authors declare that they have no known competing financial interests or personal relationships that could have appeared to influence the work reported in this paper.

7. Data availability

The raw/processed data required to reproduce these findings cannot be shared at this time as the data also forms part of an ongoing study.

References

1. Martinsen K, Hu SJ, Carlson BE. Joining of dissimilar materials. CIRP Annals - Manufacturing Technology 2015;64(2):679–99. doi:10.1016/j.cirp.2015.05.006.

2. Naidich YV, Zhuravlev VS, Gab II, Kostyuk BD, Krasovskyy VP, Adamovskyy AA, et al. Liquid metal wettability and advanced ceramic brazing. Journal of the European Ceramic Society 2008;28(4):717–28. doi:10.1016/j.jeurceramsoc.2007.07.021.

3. Asthana R, Sobczak N. Wettability, Spreading, and Interfacial Phenomena in High-Temperature Coatings. JOM: the journal of the Minerals, Metals & Materials Society 2000;52.

4. Carter CB, Norton MG. Ceramic materials: Science and engineering. Second edition ed.; New York: Springer; 2013. ISBN 978-1-4614-3522-8.

5. Horcher A, Tangermann-Gerk K, Krenkel W, Schafföner S, Motz G. Advanced ceramic coatings on aluminum by laser treatment of filled organosilazane-based composites. Ceramics International 2022;48(16):23284–92. doi:10.1016/j.ceramint.2022.04.314.

6. Atil HB, Leonhardt M, Grant RJ, Barrans S. Microstructure and mechanical properties of aluminium alloy coatings on alumina applied by friction surfacing. Proceedings of the Institution of Mechanical Engineers, Part L: Journal of Materials: Design and Applications 2021;235(2):366–84. doi:10.1177/1464420720965614.

7. Budgett HM. The adherence of flat surfaces. Proceedings of the Royal Society of London Series A: Mathematical, Physical and Engineering Sciences 1911;86(583):25–35. doi:10.1098/rspa.1911.0077.

8. Miyoshi K, Abel PB. Adhesion, Friction, and Wear in Low-Pressure and Vacuum Environments. In: Totten GE, editor. ASM Handbook. Materials Park, Ohio: ASM International. ISBN 978-1-62708-192-4; 2017, p. 362–71. URL: https://www.asminternational.org/documents/10192/22533690/05510G_SampleArticle.pdf/b3b6f3d2-813e-84b8-eed4-4ae7d5acc50e. doi:10.31399/asm.hb.v18.a0006375.

9. Popov VL. Kontaktmechanik und Reibung. Berlin, Heidelberg: Springer Berlin Heidelberg; 2010. ISBN 978-3-642-13301-5. doi:10.1007/978-3-642-13302-2.

10. Lipkin DM, Israelachvili JN, Clarke DR. Estimating the metal-ceramic van der Waals adhesion energy. Philosophical Magazine A 1997;76(4):715–28. doi:10.1080/01418619708214205.

11. Deng K, Yu Z, Zhou J, Liu H, Zhang S. Atomistically derived metal–ceramic interfaces cohesive law based on the van der Waals force. Engineering Fracture Mechanics 2013;111:98–105. doi:10.1016/j.engfracmech.2013.09.007.

12. Mirlashari . Friction surfacing onto ceramics. Connect 2009;URL: https://www.twi-global.com/media-and-events/connect/2009/july-august-2009/friction-surfacing-onto-ceramics.

13. Chmielewski T, Hudycz M, Krajewski A, Sałaciński T, Skowrońska B, Świercz R. Structure Investigation of Titanium Metallization Coating Deposited onto AlN Ceramics Substrate by Means of Friction Surfacing Process. Coatings 2019;9(12):845. doi:10.3390/coatings9120845.

14. Gandra J, Krohn H, Miranda RM, Vilaça P, Quintino L, dos Santos JF. Friction surfacing—A review. Journal of Materials Processing Technology 2014;214(5):1062–93. doi:10.1016/j.jmatprotec.2013.12.008.

15. Li W, Zhang X, Kou H, Wang R, Fang D. Theoretical prediction of temperature dependent yield strength for metallic materials. International Journal of Mechanical Sciences 2016;105:273–8. doi:10.1016/j.ijmecsci.2015.11.017.

16. Stegmueller M, Schindele P, Grant RJ. Inductive heating effects on friction surfacing of stainless steel onto an aluminium substrate. Journal of Materials Processing Technology 2015;216:430–9. doi:10.1016/j.jmatprotec.2014.10.013.

17. Bedford GM, Vitanov VI, Voutchkov II. On the thermo-mechanical events during friction surfacing of high speed steels. Surface and Coatings Technology 2001;141(1):34–9. doi:10.1016/S0257-8972(01)01129-X.

18. Stegmüller JR M, Grant RJ, Schindele P. Improvements in the process efficiency and bond strength when friction surfacing stainless steel onto aluminium substrates. Proceedings of the Institution of Mechanical Engineers, Part L: Journal of Materials: Design and Applications 2017;78:146442071770149. doi:10.1177/1464420717701494.

19. Chandrasekaran M, Batchelor A. W. , Jana S. . Study of the interfacial phenomena during friction surfacing of mild steel with tool steel and inconel. Jornal of Materials Science 1998;(33):2709–17.

20. Butt MA, Chughtai A, Ahmad J, Ahmad R, Majeed U, Khan IH. Theory of adhesion and its practical implications. A critical review. J Fac Eng Technol 2007;2008:21–45.

21. Lim CS. Untersuchung der Wechselwirkung zwischen Siliciumcarbid und den Metallen Kobalt und Nickel: Berichte des Forschungszentrums Jülich. Ph.D. thesis; Forschungszentrum Jülich, Zentralbibliothek; Jülich; 1992. URL: https://publications.rwth-aachen.de/record/74824.

22. Da Silva LFM, Öchsner A, Adams RD. Handbook of Adhesion Technology. Berlin, Heidelberg: Springer Berlin Heidelberg; 2011. doi:10.1007/978-3-642-01169-6.

23. Xin C, Liu W, Li N, Yan J, Shi S. Metallization of Al 2 O 3 ceramic by magnetron sputtering Ti/Mo bilayer thin films for robust brazing to Kovar alloy. Ceramics International 2016;42(8):9599–604. doi:10.1016/j.ceramint.2016.03.044.

24. Bach FW, Möhwald K, Bause T. Untersuchung der Einflüsse von Substratrauheit und Spritzpartikelgröße auf die Haftung thermisch gespritzter Schichten. Materialwissenschaft und Werkstofftechnik 2008;39(1):45–7. doi:10.1002/mawe.200700221.

25. Mogl J . Untersuchung und Bewertung der Metallisierung von keramischen Werkstoffen durch Reibbeschichten (Unpublished diploma thesis). University of Applied Sciences Kempten, Germany 2015;.

26. Jahanmir S, editor. Machining of ceramics and composites; vol. 53 of *Manufacturing engineering and materials processing*. New York, NY: Marcel Dekker; 1999. ISBN 082470178X. URL: http://www.loc.gov/catdir/enhancements/fy0647/98031684-d.html.

27. Ostermann F. Anwendungstechnologie Aluminium. Berlin, Heidelberg: Springer Berlin Heidelberg; 2014. doi:10.1007/978-3-662-43807-7.

28. Wessel JK. Handbook of advanced materials: Enabling new designs. Hoboken NJ: WileyInterscience; 2004.

29. Schacht M. Das Korrosionsverhalten von Werkstoffen auf Aluminiumoxid- und Zirkondioxid-Basis in wäßrigen Lösungen unter hydrothermalen Bedingungen. Forschungszentrum Karlsruhe; 1998.

30. Barat Ceramics GmbH . Material Datasheet: Aluminium oxide Al2O3. 2012.

31. Komarov SV, Romankov SE. Mechanical metallization of alumina substrate through shot impact treatment. Journal of the European Ceramic Society 2014;34(2):391–9. doi:10.1016/j.jeurceramsoc.2013.08.022.

32. Israelachvili JN. Intermolecular and surface forces. Third edition ed.; Amsterdam, Heidelberg: Elsevier; 2011. ISBN 978-0-12-391927-4.

33. Greco V, Marchesini F, Molesini G. Optical contact and van der Waals interactions: the role of the surface topography in determining the bonding strength of thick glass plates. Journal of Optics A: Pure and Applied Optics 2001;3(1):85–8. URL: https://iopscience.iop.org/article/10.1088/1464-4258/3/1/314. doi:10.1088/1464-4258/3/1/314.

34. Donaldson EC, Alam W. Surface Forces. In: Alam W, Donaldson EC, editors. Wettability. Erscheinungsort nicht ermittelbar: Gulf Professional Publishing. ISBN 9781933762296; 2006, p. 57–119. doi:10.1016/B978-1-933762-29-6.50008-9.

35. Bergström L. Hamaker constants of inorganic materials. Advances in Colloid and Interface Science 1997;70:125–69. doi:10.1016/S0001-8686(97)00003-1.

36. Freitas RA. Nanomedicine Volume I: Basic Capabilities. Austin, TX: Landes Bioscience; 1999. ISBN 157059645X.

37. Chen XJ, Levi AC, Tosatti E. Hamaker constant calculations and surface melting of metals. Surface Science 1991;251-252:641–4. doi:10.1016/0039-6028(91)91070-E.

38. Bararpour SM, Jamshidi Aval H, Jamaati R. Modeling and experimental investigation on friction surfacing of aluminum alloys. Journal of Alloys and Compounds 2019;805:57–68. doi:10.1016/j.jallcom.2019.07.010.

39. Humphreys FJ, Humphreys FJ, Hatherly M. Recrystallization and related annealing phenomena. 2. ed. ed.; Amsterdam and Heidelberg: Elsevier; 2004. ISBN 978-0-08-044164-1. URL: http://www.loc.gov/catdir/description/els051/2004556017.html.

40. Silvério S, Krohn H, Fitseva V, de Alcântara NG, Santos JFd. Deposition of AA5083-H112 Over AA2024-T3 by Friction Surfacing. Soldagem & Inspeção 2018;23(2):225–34. doi:10.1590/0104-9224/si2302.09.

41. Liu Y, Huang G, Sun Y, Zhang L, Huang Z, Wang J, et al. Effect of Mn and Fe on the Formation of Fe- and Mn-Rich Intermetallics in Al-5Mg-Mn Alloys Solidified Under Near-Rapid Cooling. Materials 2016;9(2). doi:10.3390/ma9020088.

42. Kollenberg W, editor. Technische Keramik: Grundlagen, Werkstoffe, Verfahrenstechnik. 2. ed.; Essen: Vulkan-Verl.; 2009. ISBN 978-3-8027-2953-9.

43. Imanaka Y. Multilayered Low Temperature Cofired Ceramics (LTCC) Technology. Boston, MA: Springer Science+Business Media Inc; 2005. ISBN 9780387231303. URL: http://site.ebrary.com/lib/alltitles/docDetail.action?docID=10133705. doi:10.1007/b101196.

44. Berek H, Zywitzki O, Degischer HP, Leitner H. Grenzflächenreaktionen in einer Al 2 O 3 - partikelverstärkten 6061 Al-Legierung / Interface Reactions in an Al 2 O 3 Particle Reinforced 6061 Al Alloy. International Journal of Materials Research 1994;85(2):131–3. doi:10.1515/ijmr-1994-850212.

45. Zhou Z, Fan Z, Peng HX, Li DX. High-resolution electron microscope observation of interface microstructure of a cast Al-Mg-Si-Bi-Pb(6262)/Al2O3p composite. Journal of microscopy 2001;201(2):144–52. doi:10.1046/j.1365-2818.2001.00834.x.

46. Yu Z, Wu G, Jiang L, Sun D. Effect of coating Al2O3 reinforcing particles on the interface and mechanical properties of 6061 alloy aluminium matrix composites. Materials Letters 2005;59(18):2281–4. doi:10.1016/j.matlet.2004.06.080.

47. Ojovan MI, Lee WE. Connectivity and glass transition in disordered oxide systems. Journal of Non-Crystalline Solids 2010;356(44-49):2534–40. doi:10.1016/j.jnoncrysol.2010.05.012.

48. Wilson TW. Processing, Structure, and Properties of Amorphous Aluminum Alloys: PhD diss., University of Tennessee. 2008. URL: http://etd.utk.edu/2008/WilsonTimothy.pdf.

49. Suryanarayana C. Mechanical Alloying: A Novel Technique to Synthesize Advanced Materials. Research (Washington, DC) 2019;2019:4219812. URL: https://downloads.spj.sciencemag.org/research/2019/4219812.pdf. doi:10.34133/2019/4219812.

List of Tables

List of Figures